

Effect of heating process on the ignition behavior of fine iron particles—A theoretical analysis

XiaoCheng Mi

Department of Mechanical Engineering, Eindhoven University of Technology
Eindhoven, the Netherlands

1 Introduction

The *Iron Power Cycle* has been proposed as a new solution for sustainable, long-distance transport and long-term storage of clean energy. Iron powder (i.e., particles with diameter of $\mathcal{O}(10\ \mu\text{m}-100\ \mu\text{m})$) can be burned in air to produce heat and power, and the resulting combustion product, iron-oxide powder, can be nearly 100% recycled and reduced back to iron using energy from renewable sources. Because it is non-toxic, non-corrosive, and has a low risk of explosion, iron powder has the potential to perform better than many other carbon-free energy carriers, such as hydrogen and ammonia.

To date, several industrial-scale pilot iron-powder combustors (100 kW-1 MW) have been built and tested around the world. However, this new technology currently faces the challenge of achieving a high overall oxidation degree during combustion. Based on lab-scale experiments [1], the author's group at Eindhoven University of Technology has recently identified that the main cause of the overall insufficient oxidation degree of an iron-powder combustor is primarily due to *a significant number of particles failing to ignite*. This finding suggests that achieving a high ignition rate would greatly improve the combustion performance of iron-powder burners. To achieve this goal, we must ask ourselves: How well do we truly understand the ignition mechanism and characteristics of iron particles?

1.1 Background knowledge and outstanding question on the ignition of iron particles

Mi *et al.* [2] first hypothesized that the ignition behavior of iron particle is determined by the interaction between the solid-phase oxidation rate of iron and the heat exchange between the particle and the surrounding gas. They developed a model describing the solid-phase oxidation rate of iron following a parabolic rate law, suggesting that the oxidation process is primarily controlled by the ion diffusion through an oxide shell growing on the iron surface. The kinetic parameters in this model were calibrated using experimental data on oxide-layer growth rates measured by Paidassi in the 1950s [3].

Using this model, Mi *et al.* [2] predicted the ignition temperature, T_{ign} defined as the minimum surrounding gas temperature required to trigger thermal runaway for an iron particle with a sufficiently thin initial oxide shell in air. Their model estimated T_{ign} to be approximately 1080 K across a size range from 10 to 100 μm , independent of O_2 concentration in the gas phase, assuming the particle is initially at the same temperature as the surrounding gas. To date, this prediction has been closely validated by three independent experimental studies [4–6] within the corresponding range of uncertainty, consistently indicating that gas temperatures above 1180 K can reliably ensure ignition. This finding suggests a seemingly straightforward solution to maximize the ignition rate in real-world combustors: Maintain

a gas temperature inside the combustion chamber above 1180 K. However, in practice, the situation is more complex.

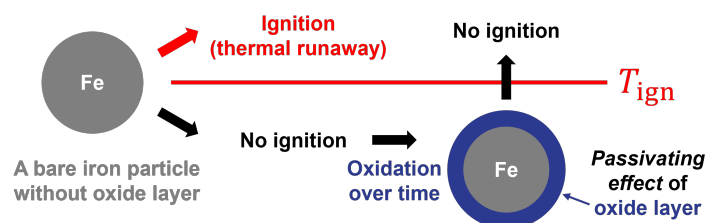


Figure 1: Illustration of a hypothetical thought experiment considering two scenarios for a bare iron particle without an oxide layer injected into a combustion chamber: (Top) Gas temperature is above T_{ign} and (Bottom) gas temperature is below T_{ign} . In the second scenario, the formation of an oxide layer has a *passivating effect* on the ignition propensity of the iron particle.

Due to heat transfer to the cooling or heat exchange system, it is unlikely that the gas temperature in a combustion chamber remains uniformly above 1180 K. Cold regions with temperatures below the ignition threshold and significant temperature gradients are likely present in a real-world combustor. Consider an iron particle initially at room temperature with a surface barely covered by oxide, injected into the combustion chamber. Two scenarios, as illustrated in Fig. 1, may occur:

1. If the gas temperature surrounding the particle is initially above T_{ign} and does not drop below this threshold, the particle can ignite, provided it has sufficient residence time.
2. If the particle is injected into a region where the gas temperature (T_g) is below T_{ign} and remains in this sub-critical temperature region for a sufficiently long time, an oxide layer will form on the particle surface, increasing the ignition temperature required for the particle. In other words, the accumulated oxide layer has a *passivating effect* on further oxidation and ignition propensity of the iron particle.

This hypothetical thought experiment suggests that the heating process, or the rate of change in gas temperature around the particle, likely affects its ignition behavior. This raises the question of how the heating process influences the ignition behavior of iron particles. In this study, the author addresses this question through a theoretical analysis based on a previously developed iron-particle ignition model [2]. Additionally, a theoretical framework is provided to help engineers design practical combustors that ensure the heating conditions required for iron-particle ignition.

2 Iron-particle ignition model

2.1 Iron oxidation kinetic model

Microscopic cross-section views of a solid-phase oxide scale grown on iron under isothermal conditions (over a range in temperature from 973 K to 1523 K) in air were first obtained by Païdassi in the 1950s. [3]: An iron-oxide scale consists of three compact layers of hematite (Fe_2O_3), magnetite (Fe_3O_4), and wüstite (FeO) stacked from the gas-oxide interface to the oxide-iron interface. The relative thicknesses of the Fe_2O_3 , Fe_3O_4 , and FeO layers with respect to the total thickness of the oxide scale are 1%, 4%, and 95%, respectively. The processes underlying solid-phase iron oxidation are conceptually illustrated in Fig. 1 of Ref. [2].

For a sufficiently thick oxide scale, the growth rate of each layer is controlled by the diffusion of ions subjected to the equilibrium activities of Fe and O at the interfaces [7]. Considering the fact that the transport of electrons and the establishment of local equilibria at the interfaces are significantly more rapid than the diffusion of ions across the oxide layers, Wagner's theory [8] relates the oxide growth rate to the diffusivity of ions. The growth of the FeO layer is the most rapid due to the fact that the diffusion coefficient of Fe cations in FeO is greater than that in Fe₃O₄ or Fe₂O₃. Such a diffusion-controlled growth follows a parabolic rate law,

$$\frac{dX_i}{dt} = \frac{k_{p,i}}{X_i} \quad (1)$$

where X_i is the thickness of an oxide layer, $k_{p,i}$ is the parabolic rate constant, and i is the index of each oxide layer. As the activities of Fe and O at the Fe-FeO, FeO-Fe₃O₄, and Fe₃O₄-Fe₂O₃ interfaces are fixed by the phase equilibria, the growth of FeO and Fe₃O₄ are barely affected by the ambient O₂ concentration [7]. The temperature dependence of $k_{p,i}$ can be described by an Arrhenius function with the values of pre-exponential factor $k_{0,i}$ and activation temperature $T_{a,i}$ for the growth of FeO and Fe₃O₄ layers that are calibrated via line fitting to the plotted data points as reported in Ref. [2].

2.2 Model of iron-particle ignition

In the current analysis, a thermophysical model based on the mass and energy balance equations with the empirically calibrated kinetic model of iron oxidation is used to describe the ignition process of an isolated iron particle, which is conceptually illustrated in Fig. 3(a) of Ref. [2]. The detailed formulation and major assumptions made in this model can be found in [2]. Note that the extension to include the curvature effect on the growth rate of an oxide layer on a spherical particle, which was first introduced by Jean-Philippe *et al.* [9], is also considered in this study.

3 Analysis results and discussion

It is important to first clarify the definition of ignition temperature in this analysis: T_{ign} is the minimum gas temperature required for an isolated iron particle with a known initial temperature and oxide layer thickness to undergo thermal runaway.

3.1 Results and findings for the hypothetical scenario—Enhancement of the passivating effect over time when $T_g < T_{\text{ign}}$

Recall the hypothetical thought experiment illustrated in Fig. 1. In this subsection, numerical tests and results are presented. The first set of numerical tests are cases with an isolated iron particle of three different sizes ($d_{p,0} = 50 \mu\text{m}$, $100 \mu\text{m}$, and $200 \mu\text{m}$) with $\delta_0 = 0.001$ and $T_{p,0} = 300 \text{K}$ exposed to a fixed gas temperature, $T_g = 1100 \text{K}$, below the initially required T_{ign} . Note that the ratio between the oxide-layer thickness and particle radius is denoted as δ and defined as $\delta = (X_{\text{FeO}} + X_{\text{Fe}_3\text{O}_4})/(r_p)$, where X_{FeO} and $X_{\text{Fe}_3\text{O}_4}$ are thickness of FeO and Fe₃O₄ layers, respectively. As results in all these cases, the particle cannot be ignited while oxide layer grows over time.

Figure 2(a)-(c) shows the time histories of particle temperature (T_p), ratio between oxide-layer thickness and particle radius (δ), and required T_{ign} over a period of 3 s. As the gas temperature 1100 K is close to the initially required ignition temperature that is approximately 1140 K, it can be seen in all three cases with different particle sizes that T_p (plotted as solid black curve) can exceed T_g (plotted as the solid blue line) for a certain period although thermal runaway does not eventually occur. This ‘‘hump’’ in

T_p over T_g is known as the *Zeldovich interval*. The occurring time of this hump increases with particle size owing to a longer preheating time required to reach the corresponding temperature range. Upon T_p reaching its peak value, the oxide layer thickness characterized by δ exhibits a rapid increase. Thereafter, δ continues to increase but at a significantly slower rate. It can also be noticed that the increase in δ is slower for larger particles.

The red curves plotted in Fig. 2(a)–(c) indicate how the required T_{ign} increases over time. The longer an iron resides in an oxidizing environment at $T_g < T_{\text{ign}}$, the higher T_{ign} is required for the particle to be ignited. These results quantitatively elucidate that the passivating effect on the ignition behavior of iron particles is continuously enhanced as the oxide layer grows over time. In Fig. 2(d), the increases in required ignition temperature (ΔT_{ign}) over time for iron particles of different sizes exposed two different gas temperatures, $T_g = 1100$ K (solid curves) and $T_g = 1120$ K (dashed curves), both below T_{ign} , are compared. For the same residence time, the increase in T_{ign} for smaller particles is greater than that for larger particles. In other words, the passivating effect is more pronounced for smaller particles given the same T_g and residence time. Further, it can be noticed that, at a slightly higher gas temperature, $T_g = 1120$ K (results plotted as dashed curves), the increase in T_{ign} is faster for all particle sizes, which is a somehow counter-intuitive finding. This is due to the fact that, as long as $T_g < T_{\text{ign}}$, a higher T_g cannot trigger thermal runaway, but results in a higher T_p and thus a faster oxide-layer growth rate, leading to a more pronounced passivating effect.

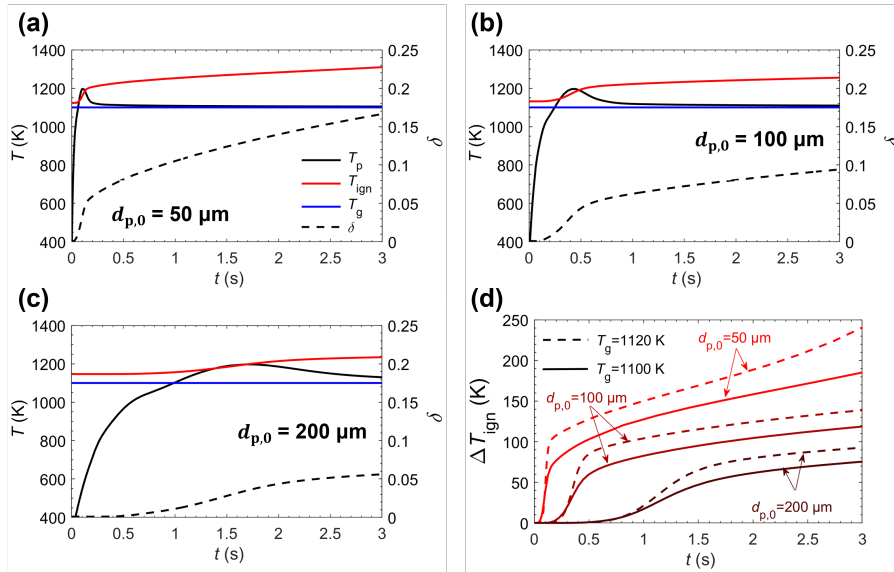


Figure 2: Numerical results of the hypothetical thought experiment—an iron particle exposed to a fixed gas temperature below T_{ign} : Time histories of particle temperature (T_p), ratio between oxide-layer thickness and particle radius (δ), and required T_{ign} for iron particle with $\delta_0 = 0.001$, $T_{p,0} = 300$ K, and (a) $d_{p,0} = 50 \mu\text{m}$, (b) $100 \mu\text{m}$, and (c) $200 \mu\text{m}$ in air at $T_g = 1100$. (d) Increase in required ignition temperature (ΔT_{ign}) over time for iron particles of different sizes exposed two different gas temperatures, $T_g = 1100$ K (solid curves) and $T_g = 1120$ K (dashed curves), below T_{ign} .

3.2 Implications of the findings on improving ignition rate of iron particles

Based on the findings from the numerical tests, the implications are qualitatively discussed in this subsection with aid of a theoretical frame. First, consider a simplified picture of a combustion chamber with an injection of iron particles as illustrated in Fig. 3 (a). Depending on the geometric configuration

of the injector, initial speed, and flow field inside the chamber, an injected iron particle travels through the chamber at a particle velocity that varies with time, $u_p(t)$. Due to the heat loss and transfer to heat exchangers, the gas temperature inside the combustion chamber is non-uniform, thus, a steady gas temperature field, $T_g(x)$, is considered. Thus, the time rate of change in gas temperature experienced by an injected particle can be described as

$$\frac{dT_g}{dt}_p = \nabla T_g \cdot u_p(t). \quad (2)$$

The gas temperature gradient field ∇T_g (or temperature field itself) and particle velocity can be controlled by specific design features of the combustor, e.g., geometry, use of pilot flames, intra-chamber heat exchangers, exhaust gas circulation (EGR). Equation 2 shows how these parameters are linked to $\frac{dT_g}{dt}_p$ that can be analyzed within the theoretical framework proposed below.

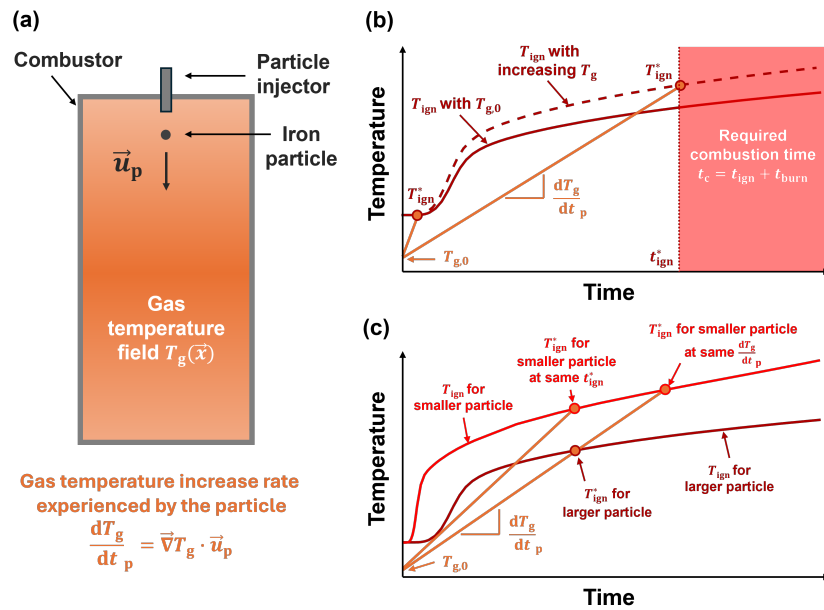


Figure 3: (a) A simplified schematic of a combustion chamber with iron-particle injection and a non-uniform field of gas temperature. Qualitative plots showing the increase in T_{ign} over time (b) for a fixed gas temperature at that initially experienced by the particle (solid curve) and for an increasing T_g experienced by the particle (dashed curve) and (c) for two different particle sizes.

Figure 3(b) shows qualitatively how the required T_{ign} increases over time for a fixed gas temperature at that initially experienced by the particle, $T_{g,0}$, plotted as the solid curve, and for an increasing T_g experienced by the particle, plotted as the dashed curve. Having $T_g > T_{ign}$ at a certain time is required for ignition to occur. However, this condition is necessary, but not sufficient. The gas temperature surrounding the particle has to be maintained at or above the required T_{ign} for a sufficiently long time for the ignition to occur. Further, to guarantee full combustion, the residence time has to be longer than the sum of ignition delay time (t_{ign}) and burn time (t_{burn}), which is herein defined as the required combustion time.

Very likely, $T_{g,0}$ at the particle injection is lower than that at the center of the chamber and the initially required T_{ign} . Thus, as indicated by the two straight lines representing the increase of T_g experienced by the particle, a faster $\frac{dT_g}{dt}_p$ is required to reduce the passivating effect of a growing oxide layer on ignition, resulting in a lower required T_{ign} and a shorter ignition onset time (t_{ign}^*). For a given set of $T_{g,0}$

and $\frac{dT_g}{dt_p}$ as a function of time, the current analysis (based on Mi *et al.*'s model [2]) can quantitatively estimate both t_{ign}^* and t_{ign} . The burn time for low O_2 concentrations in the gas phase (such as in air or lower) can be reasonably estimated for engineering purposes using models [10] that assume external transport of O_2 is the main factor limiting the oxidation rate of an ignited iron-particle. Alternatively, it can be estimated using empirical correlations provided by Ning *et al.* [11, 12] based on laser-ignited single-particle experiments. This approach establishes a theoretical framework that connects the basic principles and experimental data of iron-particle ignition and combustion with the design parameters of practical iron-powder combustors.

Further, as shown in Fig. 3(c), the increase in required T_{ign} is faster for smaller particles. As a result, to maintain the same ignition onset time (t_{ign}^*), smaller particles require a more rapid $\frac{dT_g}{dt_p}$. If $\frac{dT_g}{dt_p}$ is the same, then smaller particles require a higher T_{ign} . However, this does not mean that it is easier to ignite larger particles as they undergo a longer ignition delay (t_{ign}), suggesting that the required residence time equal or above T_{ign} is longer for larger particles.

4 Summary

This study is focused on how the heating process influences the critical phenomenon of iron-particle ignition. The hypothetical scenario that, when an iron particle is exposed to a gas medium at a temperature lower than the initially required ignition temperature, the growing oxide layer can have a passivating effect on iron oxidation, thus, hindering the ignition propensity of the particle, is numerically examined. The results show that, for an iron particle exposed to a gas temperature slightly below the the initially required T_{ign} around 1140 K, over a residence time of three seconds, the required ignition temperature increases by approximately 80 to 250 K for particle sizes ranging from 200 to 50 μm , respectively. For the same residence time, the passivating effect is more pronounced for smaller particles. Based on these results, a theoretical framework that connects the basic principles and experimental data of iron-particle ignition and combustion with the design parameters of practical iron-powder combustors is established in order to improve the ignition rate.

References

- [1] K. Zhang, "Characterization of iron powder from different streams as fuel for the iron power cycle," Metalot and Eindhoven University of Technology, Tech. Rep., 2024, (Internal internship report).
- [2] X. Mi, A. Fujinawa, and J. Bergthorson, "A quantitative analysis of the ignition characteristics of fine iron particles," *Combustion and Flame*, vol. 240, p. 112011, 2022. [Online]. Available: <https://www.sciencedirect.com/science/article/pii/S001021802200030X>
- [3] J. Païdassi, "Sur la cinetique de l'oxydation du fer dans l'air dans l'intervalle 700-1250°C," *Acta Metallurgica*, vol. 6, no. 3, pp. 184–194, 1958.
- [4] M. Abdallah, Y. Shoshin, G. Finotello, and L. de Goey, "Iron particles ignition in different hot coflow temperatures," *Proceedings of the Combustion Institute*, vol. 40, no. 1-4, p. 105261, 2024.
- [5] D. Ning, Y. Li, T. Li, B. Böhm, and A. Dreizler, "Size-resolved ignition temperatures of isolated iron microparticles," *Combustion and Flame*, vol. 270, p. 113779, 2024.
- [6] L. Cen, Z. Lyu, Y. Qian, W. Zhong, and X. Lu, "A detailed experimental and numerical study on the ignition temperature of single micron-sized spherical iron particles," *Combustion and Flame*, vol. 272, p. 113909, 2025.

- [7] D. Young, *High temperature oxidation and corrosion of metals*. Elsevier, 2008, vol. 1.
- [8] C. Wagner, "Beitrag zur theorie des anlaufvorgangs," *Zeitschrift für Physikalische Chemie*, vol. 21B, no. 1, pp. 25–41, 1933.
- [9] J. Jean-Philippe, A. Fujinawa, J. Bergthorson, and X. Mi, "The ignition of fine iron particles in the knudsen transition regime," *Combustion and Flame*, vol. 255, p. 112869, 2023. [Online]. Available: <https://www.sciencedirect.com/science/article/pii/S001021802300250X>
- [10] A. Fujinawa, L. C. Thijs, J. Jean-Philippe, A. Panahi, D. Chang, M. Schiemann, Y. A. Levendis, J. M. Bergthorson, and X. Mi, "Combustion behavior of single iron particles, part ii: A theoretical analysis based on a zero-dimensional model," *Applications in Energy and Combustion Science*, vol. 14, p. 100145, 2023. [Online]. Available: <https://www.sciencedirect.com/science/article/pii/S2666352X23000341>
- [11] D. Ning, Y. Shoshin, J. van Oijen, G. Finotello, and L. de Goey, "Burn time and combustion regime of laser-ignited single iron particle," *Combustion and Flame*, vol. 230, p. 111424, 2021. [Online]. Available: <https://www.sciencedirect.com/science/article/pii/S0010218021001607>
- [12] D. Ning, T. Hazenberg, Y. Shoshin, J. van Oijen, G. Finotello, and L. de Goey, "Experimental and theoretical study of single iron particle combustion under low-oxygen dilution conditions," *Fuel*, vol. 357, p. 129718, 2024. [Online]. Available: <https://www.sciencedirect.com/science/article/pii/S0016236123023323>